NANO LETTERS

2006
Vol. 6, No. 4
611−615

Nanoparticle-Templated Assembly of Viral Protein Cages

Chao Chen,[†,#] Marie-Christine Daniel,[†,#] Zachary T. Quinkert,[†] Mrinmoy De,[‡] Barry Stein,[§] Valorie D. Bowman,[||] Paul R. Chipman,[||] Vincent M. Rotello,[‡] C. Cheng Kao,[⊥] and Bogdan Dragnea*[,†]

Department of Chemistry, Indiana University, Bloomington, Indiana 47405, Department of Chemistry, University of Massachusetts-Amherst, Amherst, Massachusetts 01002, Indiana Molecular Biology Institute, Indiana University, Bloomington, Indiana 47405, Department of Biological Sciences, Purdue University, West Lafayette, Indiana 47907, Department of Biochemistry & Biophysics, Texas A&M University, College Station, Texas 77843

Received January 14, 2006; Revised Manuscript Received March 1, 2006

ABSTRACT

Self-assembly of regular protein surfaces around nanoparticle templates provides a new class of hybrid biomaterials with potential applications in medical imaging and in bioanalytical sensing. We report here the first example of efficiently self-assembled virus-like particles (VLPs) having a brome mosaic virus protein coat and a functionalized gold core. The present study indicates that functionalized gold particles can initiate VLP assembly by mimicking the electrostatic behavior of the nucleic acid component of the native virus. These VLP constructs are symmetric, with the protein stoichiometry and packaging properties indicating similarity to the icosahedral packing of the capsid. Moreover, a pH-induced swelling transition of the VLPs is observed, in direct analogy to the native virus.

Two-dimensional crystalline arrays of proteins self-assembled on flat supports have recently emerged as prime candidates for biotechnological applications.[1,2] Due to their intrinsic symmetry, these arrays can provide high density and equivalent environments for binding domains, characteristics that are difficult to achieve by any other technologies.[3] The ability to engineer specific regulatory switches into proteins by use of recombinant DNA technology also promises additional uses in these arrays.

The protein coat, or capsid, of many viruses provides a discrete analogue to extended protein assemblies on planar surfaces. As a consequence, modified-virus capsids have been proposed as versatile biomolecular platforms for displaying engineered peptide sequences for triggering specific host responses.[3,4] Moreover, the regular motif of tubular or quasi-spherical capsids has been used for the templated synthesis of nanomaterials ranging from magnetic particles[5] to nanowires for electronic applications.[6]

The majority of current studies on protein cage-based materials have focused on the use of the capsid surface as a nucleator and/or template for the growth or attachment of inorganic entities. The converse approach of using inorganic particles to nucleate viral capsids represents a new method for synthesizing hybrid inorganic/viral particles, thus widening the range of possible combinations of physical and chemical properties.

Preliminary experiments on the encapsulation of functionalized gold nanoparticles into brome mosaic virus (BMV) capsids have shown that the VLP protein coat is likely organized in a closed shell, similar in its physicochemical properties to the native virus.[7,8] These previous examples of nanoparticle encapsidation were characterized by an extremely low yield relative to the formation of empty capsid (∼1%),[9] in stark contrast with the essentially quantitative in-vivo incorporation of the native RNA.[9] Practical application of these systems, however, requires a high yield of homogeneous material. Moreover, knowledge of the VLP shell structure and concomitant preservation of its functional attributes also requires homogeneous materials that can be used for high-resolution structural studies.

The fact that empty capsids can be obtained in vitro in the absence of BMV−RNA but are rarely observed in-vivo indicates that the nucleic acid acts as a heterogeneous nucleation site for the capsid. The question is therefore: what surface properties are required for an inorganic particle to mimic the RNA nucleation of the native virus, providing

* Corresponding author: dragnea@indiana.edu.
[†] Department of Chemistry, Indiana University.
[‡] University of Massachusetts-Amherst.
[§] Indiana Molecular Biology Institute, Indiana University.
[||] Purdue University.
[⊥] Texas A&M University.
[#] These authors have contributed equally.

10.1021/nl0600878 CCC: $33.50
Published on Web 03/15/2006

analogous efficiency of capsid self-assembly and particle incorporation? The present paper is a first attempt at answering this question. We report a new methodology for gold nanoparticle encapsidation that provides a yield of incorporation greater than 95%. The VLPs thus obtained are homogeneous by transmission electron microscopy and dynamic light scattering and can be produced in scalable fashion, free of both protein aggregates and empty capsids.

Previous attempts to encapsulate Au nanoparticles functionalized with citrate or streptavidin into BMV capsids were modeled after the protocol for in-vitro reassembly of Cowpea Chlorotic Mottle Virus, where viral RNAs formed the core.[8,10] The yield of encapsulation in these systems has been empirically defined as the ratio between the number of gold-containing capsids and the total number of quasi-spherical aggregates composed of empty and gold-containing capsids. The yield of incorporation was found to depend on the size of the gold nanoparticle and on the surface moiety. However, in all cases it remained below 2−3%.[8]

Two primary reasons were believed to be responsible for the low incorporation yield in the previous protocol. First, the concentration of Au nanoparticles was less than 2% of the stoichiometric amount for the encapsulation reaction. Higher Au particle concentrations, however, resulted in irreversible aggregation of the nanoparticles during the change in pH and ionic strength required by the protocol. The second limitation was that the assembly of empty capsids competed with the formation of VLPs due to inefficiency of the Au/citrate particles at nucleation and/or propagation of the assembly process.

Experimental evidence from surface plasmon resonance (SPR) shifts and tryptophan fluorescence quenching indicated that although a fast initial complexation between protein dimers and gold did occur, the subsequent growth does not compete efficiently with the formation of empty capsids. Therefore, efficient growth of a capsid from an initial protein/particle condensate is likely to require a well-defined protein multimer precursor. For the citrate-stabilized and the DNA-stabilized gold particles previously used, hydrophobic interactions between the protein and the metal core are possible.[9] These interactions could affect the structure of the hypothetical required precursor for rapid growth. Therefore, although gold−protein complexes form, the growth into VLPs is a low-probability event and the formation of empty capsids is therefore kinetically favored.

Improved nanoparticle stability coupled with decreased hydrophobic interaction between the gold particle and the protein shell may be therefore required for the autocatalytic growth of a VLP to take place. We have thus investigated ligands that should satisfy both the negative charge and the stability conditions required for self-assembly. Carboxylate-terminated thiolalkylated tetraethylene glycol (TEG) **1** (Figure 1) fulfils both of these requirements. The strongly hydrophilic TEG is resistant to nonspecific binding of biomolecules.[11] The ligands have been synthesized as previously described.[12] The TEG-coated particles were obtained through ligand-exchange from citrate-coated gold particles and were designed to fill entirely the void inside the viral

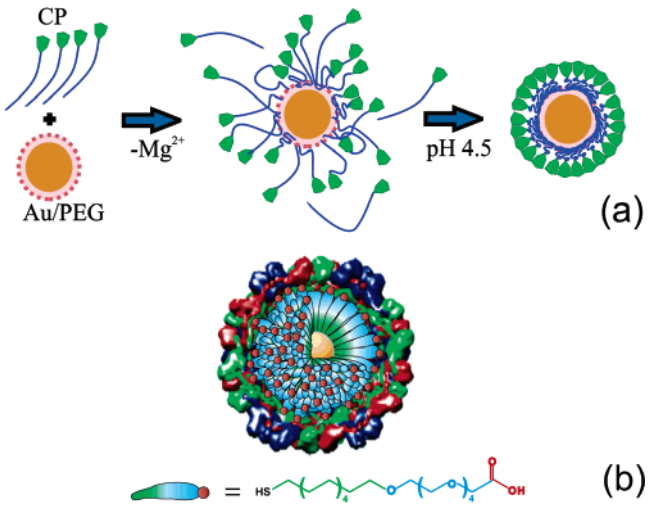

Figure 1. (a) Proposed mechanism of VLP assembly (CP = capsid protein): first, electrostatic interaction leads to the formation of disordered protein−Au nanoparticle complexes. The second step is a crystallization phase in which the protein−protein interactions lead to the formation of a regular capsid. (b) Schematic depiction of the encapsidated nanoparticle functionalized with carboxyl-terminated TEG chains.

capsid (see Supporting Information). After functionalization, the particles have a diameter of 16 ± 1.2 nm, as found by TEM. This size closely corresponds to the inner diameter of the viral BMV capsid (17−18 nm).[13]

The VLP self-assembly was modified from the previous protocol.[9] First, the gold particle concentration was significantly raised to be ∼1/180th of the stoichiometric amount of proteins. Second, a final dialysis against an acidic buffer replaced the original centrifugation step through an acidic sucrose gradient. Third, following the BMV phase diagram of Cuillel and Berthet-Colominas,[14] steps in the protocol that would allow the formation of empty capsids were avoided. More specifically, after dissociation of intact BMV viruses and purification of the protein away from the RNA, the gold sol was mixed with the BMV proteins in a pH 7.4 buffer containing high ionic strength. The mixture was then dialyzed first at pH 7.4 while lowering the ionic strength, followed by a second dialysis against a low ionic strength acidic buffer (pH 4.7).

TEG-coated and citrate-coated gold particles were both subjected to the above procedure. In addition, assembly of the capsid protein in the absence of a foreign core was also performed as a control. All of the reactions were analyzed by dynamic light scattering (see Supporting Information) and by transmission electron microscopy without further purification to allow an unbiased examination of the products. Reactions lacking gold resulted in the formation of empty capsids with sizes varying from 20 to 29 nm as well as incomplete capsids: this heterogeneity most likely arises from inefficient capsid formation under the conditions used. As expected, significant precipitation occurred during the reassembly procedure for citrate-coated particles. In contrast, precipitation was absent in the case of TEG-coated particles, indicating that the coating of the Au particle significantly affected the assembly process.

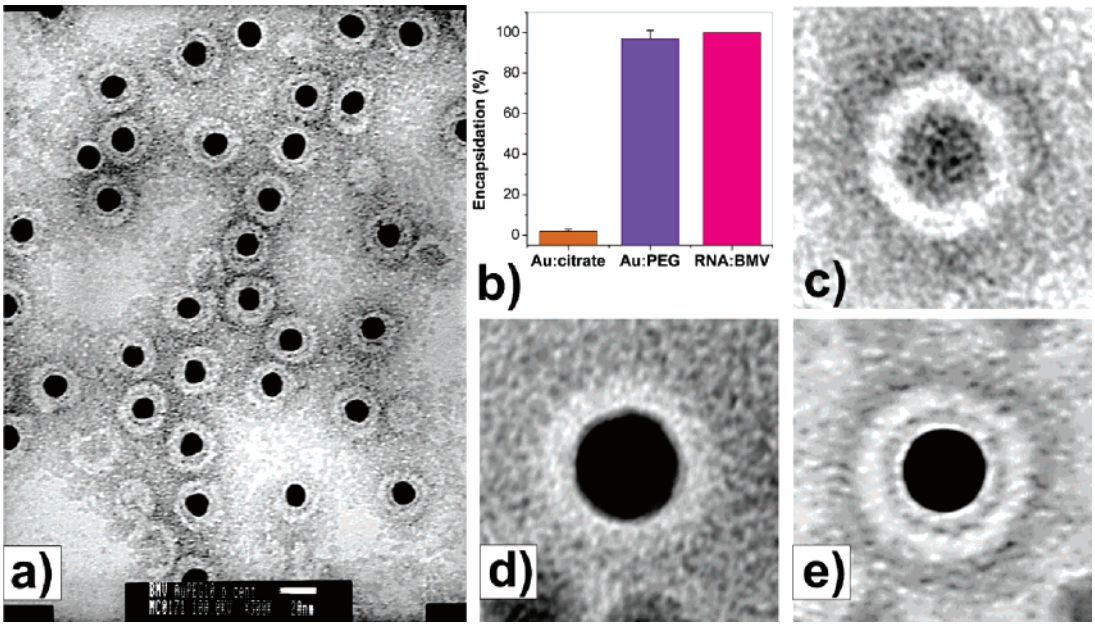

Figure 2. (a) Transmission electron micrograph of negatively stained virus-like particles obtained from functionalized gold nanoparticles (black centers, 12 nm diameter) and BMV capsid protein. (b) Comparison of encapsidation yields for citrate:Au with the previous protocol[8], Au:TEG, and native RNA. Averaged transmission electron micrograph of (c) empty BMV capsid, (d) citrate-coated VLP, and (e) TEG-coated VLP. The averages have been obtained by superposition of 10 individual images, in each case.

The TEG-coated particles had a yield of encapsulation of 95±5%, (Figure 2 a,b), in contrast to encapsidation of citrate-coated particles, which had VLPs containing Au nanoparticles at approximately 1%, consistent with previous results. Assembly solutions with the TEG-coated particles also contained a small number of empty protein shells (<3%), likely due to their inability to find a coated core. Also, incomplete shells around the TEG-gold particles were observed in very small numbers (<2%). This is in contrast with the ensemble of particles obtained from the coat protein alone, for which significantly more incomplete capsids were found. These observations support the idea that a cooperative growth process occurs in which the negatively charged particle acts to nucleate the assembly of the protein coat.

The homogeneous character of the samples enabled a morphological comparison between citrate and TEG-functionalized VLPs and the empty capsids. The pictures of 10 representative particles from each sample have been superimposed. The average size, which is 26 nm ± 2 nm, has thus been determined, regardless of the kind of gold particles used, Figure 2c−e. This size corresponds, within the experimental error, to the size of the native BMV. However, the best definition is clearly achieved for the TEG-containing VLPs (Figure 2e) and the empty capsid (Figure 2c). The more diffuse protein layers observed for the citrate-coated particles suggest that this core surface leaves the protein shell disordered, while the TEG-coated particles produce a protein shell that is more similar to the empty capsid. Analysis of the VLPs by cryoelectron microscopy supports this hypothesis. In Figure 3, the protein coat of a single VLP shows clear signs of a regular structure. Note that, in this case, the image has been taken from only one particle, without averaging. It is interesting to note that while the Au core appears to be faceted, the TEG layer buffers this constraint well enough to maintain the native quasi-spherical protein shell structure.

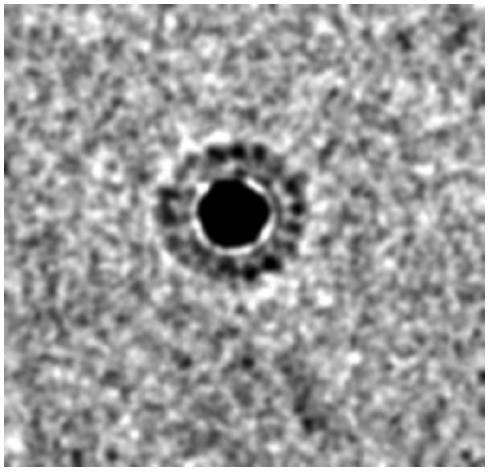

Figure 3. Cryoelectron micrograph of a single VLP. The regular character of the protein structure coating the 12 nm diameter Au nanoparticle (black disk) is evident.

The regular structure observed in Figure 3 can be achieved in many different ways: icosahedral symmetry requires that the total number of protein subunits must be an integer multiple of sixty.[15] The infectious BMV capsid has a triangulation number of T = 3, which means that there are 180 proteins forming it. Nevertheless, RNA-controlled polymorphism is known to occur. Both 180- and 120-subunit virions have been induced to assemble in vivo, when engineered mRNA is used.[16]

To determine how many protein subunits it takes to make our VLPs (Figure 3), we have used the experimental observation that incomplete VLPs will form larger structures through cohesive interactions of capsid fragments attached

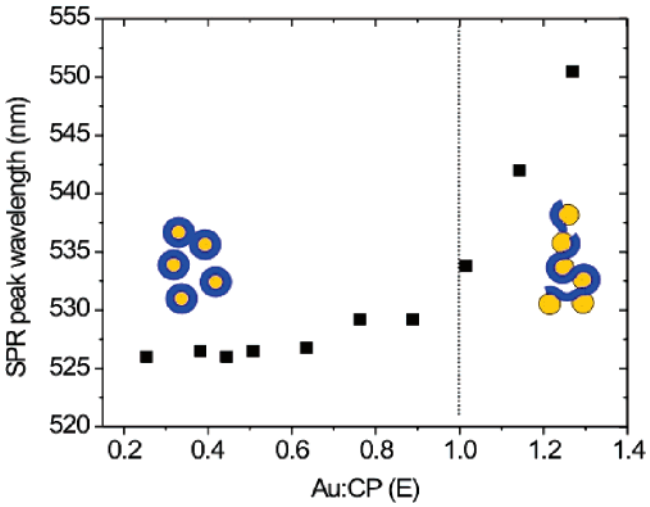

Figure 4. Determination of the Au/protein VLP stoichiometry using the position of the surface plasmon resonance (SPR) peak as a function of the ratio between the number of Au particles and capsid proteins. When Au/capsid ratios are lower than 1E, VLPs are effectively stabilized by their protein coat as indicated by a constant position of the SPR peak. The peak shifts abruptly when the gold particles are incompletely coated with protein and they become prone to aggregation. This feature allows one to estimate the number of proteins per Au particle for a complete shell.

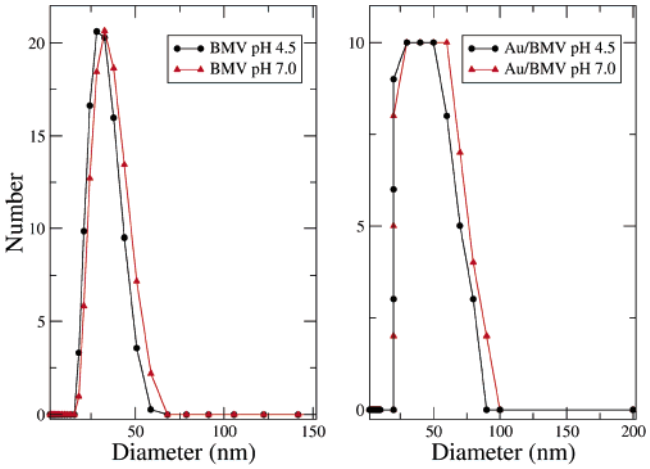

Figure 5. Dynamic light scattering observation of the swelling transition for both VLP (12 nm core) and BMV. The variation in size is small (5−6 nm), but reproducible.

to metal cores. As a result, coupling of the surface plasmon resonance occurs between the Au cores of the aggregating, incomplete VLPs. The coupling effect can be easily identified as a red shift in the peak position of the surface plasmon. Thus, for a fixed concentration of protein, a small amount of added Au leads to a clear, red product, while a large amount tends to produce aggregates recognizable due to their blue color, Figure 4.

The onset of aggregation in Figure 4 occurs for a ratio protein/Au greater close to ∼180 proteins per Au particle, which, corroborated with the diameter, implies that the symmetric VLP in Figure 3 is likely to be a T = 3 particle for the conditions used. To confirm this T-number estimate, further structural investigations by 3D image reconstruction are on their way.

The cryo-TEM, the stoichiometry, and the size distribution data, combined with the efficiency of polyanion incorporation, indicate that the VLPs prepared by the method outlined here are remarkably similar with native BMV capsids. A step further in this direction would be to assess whether the VLPs also preserve some of the functional properties of native BMV. One of the most salient BMV characteristics is the swelling transition.[17] The ∼28 nm diameter BMV capsid is most stable at low to moderate ionic strength buffers with pH lower than 5.0, but undergoes a profound structural transition when the pH is increased from 5 to 7. In presence of Mg^{2+}, which helps stabilizing the capsid at pH levels close to neutrality, reversible expansion occurs without dissociation.[17]

We have followed the reversible, pH-induced, expansion transition using dynamic light scattering for both BMV particles and VLPs, Figure 5. The difference in the DLS peak shape between the BMV and VLP samples may be due to the fact that the layered nature of the VLP is not properly accounted for by the DLS software, which may lead to a distorted hydrodynamic diameter distribution. The presence of subpopulations in the VLP sample is also a possible reason. The breath of the peak is dominated by the instrumental response function in both cases. Although close to the resolution limit of the method, a definite reversible swelling of the same magnitude as for the native BMV is observed for VLPs. Therefore, similar to native BMV, the swelling transition is a characteristic of VLP capsids, too.

To conclude, we have demonstrated a high-yielding route to homogeneous VLPs. For the first time, a regular protein layer is shown to self-organize on the surface of a nanoscopic inorganic spherical template. The new synthetic route is based on self-assembly of protein subunits around a functionalized anionic nanoparticle, providing VLPs with properties similar to the native BMV virus. Our ability to encapsulate foreign materials inside viruses should enhance their optical response and sensing capabilities. These VLPs thus provide access to materials for creation of new optical and functional probes for biomedical imaging and sensing purposes.

Acknowledgment. The authors thank Dr. Suchetana Mukhopadhyay for valuable discussions. The work has been carried out under the auspices of a grant from the National Science Foundation (BES-0322767) and of a NIH grant GM59249 (to V.R.).

Supporting Information Available: Protocols used for nanoparticle synthesis and functionalization and for VLP assembly. Control experiment of empty capsid formation through the same protocol as for the VLP assembly. This material is available free of charge via the Internet at http://pubs.acs.org.

References

(1) Clarkson, S. *Nat. Rev. Microbiol.* **2004**, *2*, 353.
(2) Sanford, K.; Kumar, M. *Curr. Opin. Biotechnol.* **2005**, *16*, 416.
(3) Khor, I. W.; Lin, T. W.; Langedijk, J. P. M.; Johnson, J. E.; Manchester, M. *J. Virol.* **2002**, *76*, 4412.

(4) Schlick, T. L.; Ding, Z. B.; Kovacs, E. W.; Francis, M. B. *J. Am. Chem. Soc.* **2005**, *127*, 3718.
(5) Allen, M.; Bulte, J. W. M.; Liepold, L.; Basu, G.; Zywicke, H. A.; Frank, J. A.; Young, M.; Douglas, T. *Magn. Reson. Med.* **2005**, *54*, 807.
(6) Mao, C. B.; Solis, D. J.; Reiss, B. D.; Kottmann, S. T.; Sweeney, R. Y.; Hayhurst, A.; Georgiou, G.; Iverson, B.; Belcher, A. M. *Science* **2004**, *303*, 213.
(7) Chen, C.; Kwak, E.-S.; Stein, B.; Kao, C. C.; Dragnea, B. *J. Nanosci. Nanotechnol.* (special issue) **2005**, *5*, 2029.
(8) Dragnea, B.; Chen, C.; Kwak, E. S.; Stein, B.; Kao, C. C. *J. Am. Chem. Soc.* **2003**, *125*, 6374.
(9) Kao, C. C.; Sivakumaran, K. *Mol. Plant. Path.* **2000**, *1*, 91.
(10) Zhao, X. X.; Fox, J. M.; Olson, N. H.; Baker, T. S.; Young, M. J. *Virology* **1995**, *207*, 486.
(11) Harris, J. M.; Zalipsky, S. *Poly(ethyleneglycol): chemistry and biological applications*; American Chemical Society: Washington, DC., 1997.
(12) Hong, R.; Fischer, N. O.; Verma, A.; Goodman, C. M.; Emrick, T.; Rotello, V. M. *J. Am. Chem. Soc.* **2004**, *126*, 739.
(13) Zulauf, M. C., M.; Jacrot, B. *NATO ASI Series, B: Physics* **1981**, *73*, 865.
(14) Berthet-Colominas, C.; Cuillel, M.; Koch, M. H. J.; Vachette, P.; Jacrot, B. *Eur. Biophys. J.* **1987**, *15*, 159.
(15) Caspar, D. L. D.; Klug, A. *Cold Spring Harbor Symposia on Quantitative Biology* **1962**, *27*, 1.
(16) Krol, M. A.; Olson, N. H.; Tate, J.; Johnson, J. E.; Baker, T. S.; Ahlquist, P. *Proc. Natl. Acad. Sci. U.S.A.* **1999**, *96*, 13650.
(17) Argos, P.; Johnson, J. E. Chemical stability in simple spherical plant viruses, in biological macromolecules and assemblies. In *Virus Structures*; Jurnak, F. A., McPherson, A., Eds.; John Wiley & Sons: New York, 1984; p 1.

NL0600878